AMERICAN SOCIETY FOR MICROBIOLOGY | Journal of Virology®

VIRUS-CELL INTERACTIONS

The Immune-Specific E3 Ubiquitin Ligase MARCH1 Is Upregulated during Human Cytomegalovirus Infection to Regulate Iron Levels

Madison Martin,[a] Praneet Sandhu,[a]* Rinki Kumar,[a] Nicholas J. Buchkovich[a]

[a]Department of Microbiology and Immunology, Penn State College of Medicine, Hershey, Pennsylvania, USA

Madison Martin and Praneet Sandhu contributed equally to this article. Author order was determined alphabetically.

ABSTRACT Human cytomegalovirus (HCMV) modulates numerous cellular pathways to facilitate infection. Iron is essential to many cellular processes and is often incorporated into proteins and enzymes involved in oxidative phosphorylation and DNA synthesis and repair, among others. Despite its prominent role in the cell, little is known about the regulation of iron metabolism during HCMV infection. Herein, we observe modulation of the transferrin receptor (TfR) during infection and a corresponding change in the cellular labile iron pool. TfR and the iron pool are increased early during infection and then return to mock levels at the late stages of infection. We identified the cellular ubiquitin ligase MARCH1 as an important regulator of TfR. MARCH1 plays a proviral role during infection, as its knockdown leads to a decrease in infectious titers. Knockdown of MARCH1 also leads to an increase in ROS, lipid peroxidation, and mitochondrial dysfunction. Inhibiting an early increase in TfR expression during infection also decreases virus production. These findings indicate the importance of tightly regulating iron metabolism during HCMV infection to facilitate efficient virus production.

IMPORTANCE Iron is essential for cells, playing important roles in energy generation, DNA replication, and gene expression. During infection, HCMV alters many cellular processes to aid its replication. We found that iron levels are tightly regulated during infection and that dysregulation of iron levels alters the ability to produce infectious virions. We also found that HCMV inactivates many of the cellular safeguards put in place to deal with excess iron. Thus, infected cells become more susceptible to variations in iron levels, which could be exploited as a therapeutic strategy for dealing with HCMV infections.

KEYWORDS HCMV, MARCH1, transferrin receptor, iron

Human cytomegalovirus (HCMV) is an opportunistic herpesvirus that causes disease in immunocompromised individuals and neonates (1, 2). There is a need to fully understand the interplay between the virus and the host to develop better therapeutic strategies for susceptible groups. Throughout the course of infection, HCMV usurps many cellular pathways to facilitate its own replication in infected cells, often by modifying the protein composition of the cell to promote viral replication. For instance, HCMV increases cellular metabolic proteins while downregulating immune effector proteins, both of which are beneficial for the virus (3, 4). Identifying cellular proteins that are essential for the viral life cycle will reveal new targets for treatment of HCMV infections.

Iron is an essential metal ion that is important for many functions at both the cellular and organismal level. Within cells, iron is incorporated into many proteins and used for its catalytic and redox reactive properties. Iron is required for several processes that

Editor Felicia Goodrum, University of Arizona

Copyright © 2022 American Society for Microbiology. All Rights Reserved.

Address correspondence to Nicholas J. Buchkovich, nbuchkovich@pennstatehealth.psu.edu.

*Present address: Praneet Sandhu, Department of Microbiology and Immunology, University of North Carolina School of Medicine, Lineberger Comprehensive Cancer Center, Chapel Hill, North Carolina, USA.

The authors declare no conflict of interest.

Received 20 October 2021
Accepted 13 January 2022
Accepted manuscript posted online 19 January 2022
Published 23 March 2022

occur within the mitochondria, including energy generation through oxidative phosphorylation, and is incorporated into proteins that carry out DNA synthesis, repair, and transcription (5, 6). Because of its requirement in these fundamental processes, iron deficiency greatly impairs cellular function. Although iron ions are crucial for cells, excess iron can also be harmful. The labile iron pool (LIP) is the cellular source of free iron that is used for incorporation into proteins, but this iron pool is also the main driver of iron-dependent oxidative stress (7). Free iron ions can react with hydrogen peroxide to form hydroxyl radicals that then generate oxidative damage that disrupts cellular functions. Through this mechanism, excess iron has been shown to lead to lipid peroxidation that initiates an iron-mediated form of cell death known as ferroptosis; thus, iron concentration must be tightly regulated (8).

Viruses rely on the proper functioning of many iron-dependent cellular processes. Accordingly, iron chelators inhibit infection of HIV-1 and some herpesviruses, including HCMV (5, 9–12). Not much is known about the regulation of iron metabolism during HCMV infection. Intracellular iron concentrations have been linked to cytomegaly, and the viral protein US2 has been shown to degrade homeostatic iron regulator (HFE), which can affect iron uptake, but little has been shown about the role of iron in viral replication and production (10, 13).

Cellular iron uptake is mainly mediated through a complex consisting of iron-bound transferrin (Tf) and the transferrin receptor (TfR). Iron-bound Tf binds to TfR on the cell surface, and the complex is internalized through receptor-mediated endocytosis. In acidified endosomes, iron is released and transported to the cytosol. While the Tf-TfR complex is recycled back to the cell membrane, iron in the cytosol is either incorporated into ferritin or becomes part of the LIP to be used in proteins. TfR expression is regulated posttranscriptionally in response to cellular iron levels by the iron response proteins (IRPs). The expression of TfR can also be posttranslationally regulated through targeted ubiquitination and lysosomal degradation mediated by MARCH (membrane-associated RING CH) E3 ligases (14, 15).

The MARCH family of E3 ubiquitin ligases were discovered as mammalian homologs to the K3 and K5 proteins of Kaposi's sarcoma herpesvirus (KSHV) (16). TfR has been identified as a target for two highly homologous MARCH ligases, MARCH1 and MARCH8 (16). While MARCH8 is ubiquitously expressed in tissue, MARCH1 expression is limited to immune cells such as dendritic cells, monocytes, and B cells, where a major target (16–19) is the MHC class II complex (16–21). Since MARCH1 promotes degradation of this antigen presenting complex, it plays an important role in shutting down the immune response and is induced by the immunosuppressive cytokine IL-10 (19, 22).

Herein, we show that levels of TfR protein and transcripts spike early in infection before returning to basal levels. One component of this regulation is increased lysosomal degradation, which is mediated by MARCH1. MARCH1, which is not normally expressed in fibroblasts, is induced during infection and is important for the production of infectious virus titers. When MARCH1 is knocked down, TfR levels remain elevated, resulting in increased levels of reactive oxygen species, an accumulation of lipid peroxidation and mitochondrial dysfunction. Further illustrating the importance of tightly regulating iron levels during HCMV infection, preventing the early increase in TfR, either by directly knocking it down or by expressing MARCH1, also decreases infectious titers. Thus, iron levels are tightly regulated during HCMV infection and disruption of this regulation impairs the production of infectious virions.

RESULTS

HCMV regulates levels of TfR during infection. Iron is essential for several processes required to produce HCMV virions. We found that the cytoplasmic LIP increases early in infection, peaking at 24 hpi, before declining back to mock levels (Fig. 1A). This is consistent with a previous study reporting a peak in LIP at 24 hpi, followed by a subsequent decrease (10). To probe the mechanism behind this iron regulation, we investigated whether HCMV alters the levels of TfR. We found that TfR protein levels were

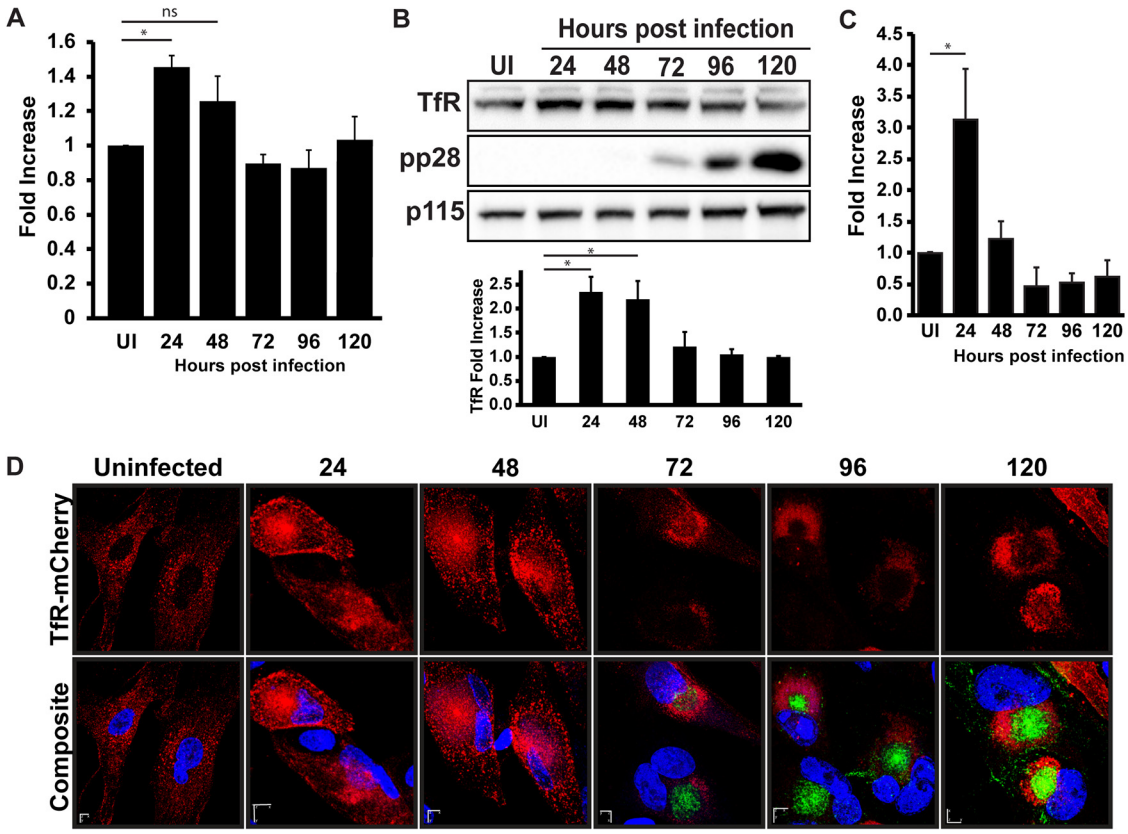

FIG 1 HCMV regulates levels of TfR during infection. (A) Labile iron pool measurements taken by measuring calcein fluorescence increase following iron chelation with isonicotinoyl salicylaldehyde hydrazone (SIH) in uninfected and HCMV-infected (TB40/E, MOI = 3) cells at 24, 48, 72, 96, and 120 hpi. Data are presented as fold increase over levels in uninfected cells. (B) Western blot analysis of lysates from uninfected or HCMV-infected fibroblasts (as in (A)) at 24, 48, 72, 96, and 120 hpi. Blots were probed for TfR and pp28, with p115 serving as a loading control. Graph below blots shows average fold increase for TfR, when compared to uninfected samples, from three independent experiments. (C) qPCR analysis of TfR transcripts isolated from uninfected or HCMV-infected fibroblasts (as in (A)) at 24, 48, 72, 96, and 120 hpi. TfR transcripts were normalized to GAPDH and reported as a fold change to the uninfected sample. (D) Fluorescence images of TfR-mCherry (red), pp28 (green), and DAPI-stained nuclei (blue) in uninfected and HCMV-infected (as in (A)) cells at 24, 48, 72, 96, and 120 hpi. X and Y scale bar = 0.12 μm, z scale bar = 0.25 μm. For the above panels, * indicates $P < 0.05$, ns = not significant, and data are average of three independent experiments.

sharply increased at 24 and 48 hpi, followed by a decline and return to mock levels (Fig. 1B). The general vesicular transport protein p115 (USO1) levels are unaltered during infection (23) and were used as a loading control. The increase in protein levels corresponded with an increase in TfR transcript levels (Fig. 1C). In addition to changing protein levels of TfR during infection, altered localization may also affect the ability of TfR to uptake iron. To assess TfR localization during infection, fibroblasts were transduced with lentivirus carrying a TfR construct tagged at the C-terminus with mCherry. Following selection, the TfR-mCherry expressing fibroblasts were plated on coverslips and infected with HCMV. Samples were fixed at 24-h increments following infection. TfR localized to the plasma membrane and puncta near the plasma membrane, presumably recycling endosomes, in uninfected cells and during the early stages of infection. In contrast, late in infection TfR is internalized to a ring surrounding the pp28-containing core of the cytoplasmic viral assembly compartment (cVAC) (Fig. 1D). The cVAC is the proposed final site of viral maturation and contains concentric layers of organelles, an endosomal core surrounded by membrane rings from the Golgi and trans-Golgi network (24–26). While the change in TfR localization may simply be a result of the altered flow of cellular membranes associated with formation of the cVAC, it likely also has implications on the ability of TfR to facilitate iron entry into cells during the late stages of infection. These TfR results correlate with the change in iron levels and

suggest that HCMV modulates cellular iron levels by regulating the levels and localization of TfR.

MARCH1, but not MARCH8, is induced during infection. Following endocytosis of the iron-Tf-TfR complex, iron is dissociated in the acidic endosome lumen and the Tf-TfR complex is recycled back to the cell surface (27). Thus, a single Tf-TfR complex can undergo multiple rounds of endocytosis and the TfR protein has a reportedly long half-life (15, 28–30). We hypothesized that HCMV may therefore promote the degradation of TfR. We found that TfR levels were increased in infected cells treated with chloroquine or concanamycin A, compounds that alter the pH of lysosomes and affect protein degradation (Fig. 2A). HCMV therefore modestly decreases TfR through degradation as part of regulating levels of the labile iron pool.

Two ubiquitin ligases of the MARCH ligase family were previously shown to target TfR for degradation, MARCH1 and MARCH8 (16). We investigated whether MARCH1 or MARCH8 were differentially regulated by HCMV. We found that while MARCH1 transcripts steadily increased as infection progressed, levels of MARCH8 transcripts were not altered at any time during infection (Fig. 2B and C). Western blot analysis confirmed a corresponding increase in MARCH1 protein, which increased with similar kinetics as the viral late protein pp28 (Fig. 2D). To ensure that this was not a strain-specific effect limited to the TB40/E strain of HCMV, we utilized another strain of HCMV (AD169) and confirmed that MARCH1 protein levels similarly increased during infection (Fig. 2E). Thus, HCMV specifically upregulates MARCH1, but not the highly homologous protein MARCH8 during infection.

The observed increase in MARCH1 was particularly interesting given it is not normally expressed in fibroblasts. Central to its role in degrading the MHC Class II complex, MARCH1 is induced by the immunosuppressive cytokine IL-10 in immune cells (19, 22). Since HCMV encodes a viral version of IL-10, UL111A, we hypothesized that the induction of MARCH1 was dependent on the expression of this viral IL-10 homologue. Utilizing a virus lacking expression of UL111A (23), we found that MARCH1 was still induced even in the absence of UL111A (Fig. 2F). The viral IL-10 was therefore not responsible for inducing MARCH1 during HCMV infection. Fibroblasts produce very little cellular IL-10, and these levels were unchanged throughout infection (Fig. 2G), in contrast to the significant increase following infection of an immune cell known to serve as a source of IL-10 (31). Thus, it is unlikely that the induction of MARCH1 during infection was due to cellular IL-10 signaling. The induction of both MARCH1 transcript and protein, however, was blocked by addition of acyclovir, suggesting that MARCH1 induction was dependent on late gene synthesis following DNA replication (Fig. 2H and I). Thus, it appears that HCMV specifically upregulates MARCH1 outside of its normal induction pathway.

MARCH1 knockdown adversely affects HCMV titers and the late stages of infection. Since HCMV specifically induces MARCH1, we hypothesized that it is required to produce infectious progeny. We utilized two different clones of shRNA to knock down MARCH1 in primary fibroblasts. This approach resulted in a substantial, but not complete, knockdown of MARCH1 (Fig. 3A). Since clone #1 resulted in a greater decrease in MARCH1 protein, it was selected for all additional analyses. Infectious titers were significantly reduced, by about one log, following infection of the knockdown fibroblasts when compared to a control infection (Fig. 3B). Thus, MARCH1 is important for producing infectious HCMV virions.

We hypothesize that MARCH1 is induced during infection to downregulate TfR, which is consistent with the kinetics of both MARCH1 induction and TfR downregulation. Thus, we expect to see a block late in infection. In the absence of MARCH1 we saw no difference in protein levels or kinetics of induction for the immediate early proteins IE1 and IE2 or the DNA polymerase processivity factor UL44 (Fig. 3C and D). Additionally, the number of genome copies were similar between control and MARCH1-knockdown fibroblasts (Fig. 3E), and electron microscopy (EM) images of infected nuclei confirmed the presence of genome-containing nucleocapsids. (Fig. 3F). Thus, MARCH1 does not affect the initiation of infection, viral DNA replication, or genome encapsidation. In contrast, protein levels of

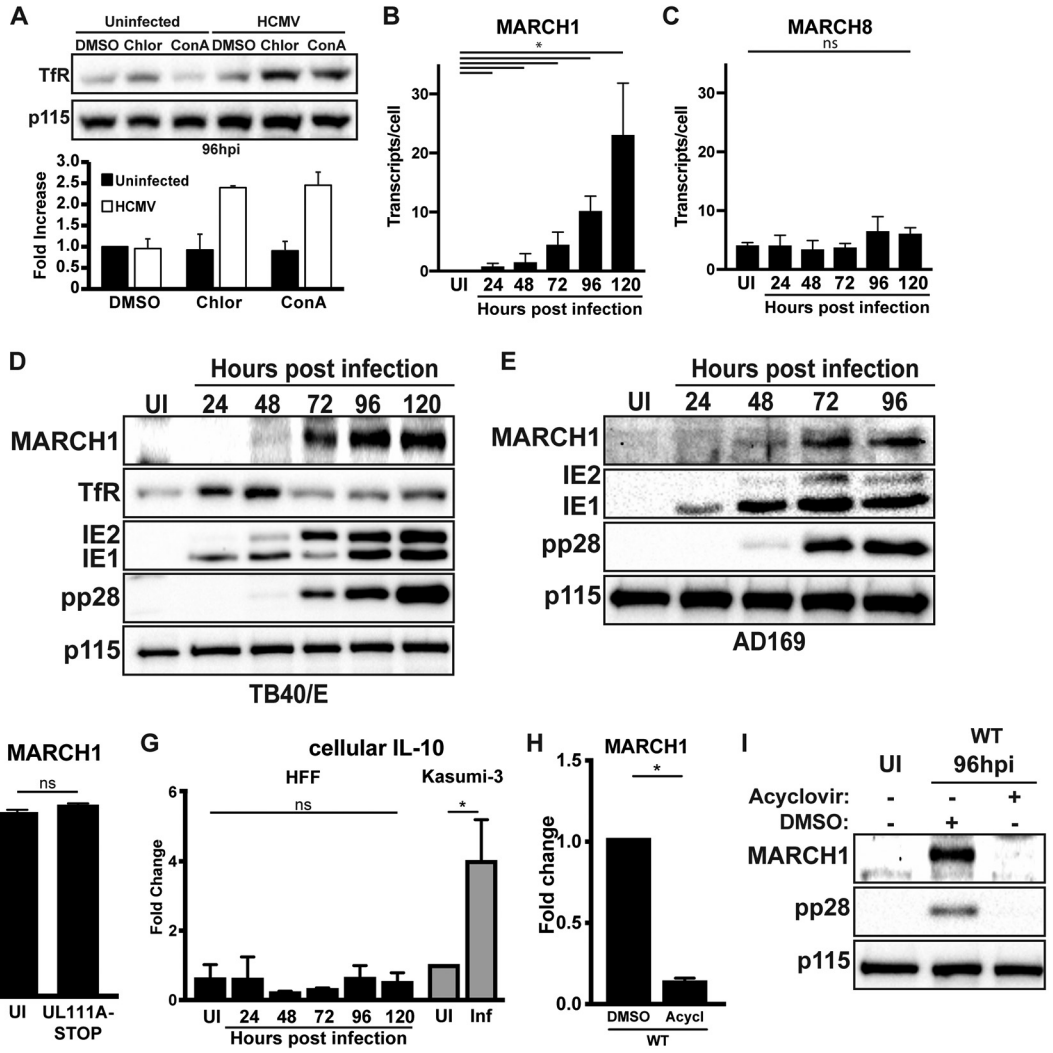

FIG 2 MARCH1, but not MARCH8, is induced during infection. (A) Lysates from uninfected or HCMV-infected cells (TB40/E, MOI = 3, 96 hpi) treated with DMSO, chloroquine (Chlor), or concanamycin A (ConA) were analyzed by Western blotting and probed for TfR and a loading control p115. Graph below blots shows average fold increase for TfR, when compared to uninfected DMSO samples, from three independent experiments. (B and C) qPCR analysis of (B) MARCH1 and (C) MARCH8 transcripts isolated from uninfected or HCMV-infected fibroblasts at 24, 48, 72, 96, and 120 hpi, reported as total number of transcripts per cell. (D and E) Western blot analysis of lysates from uninfected fibroblasts or fibroblasts infected with (D) TB40/E or (E) AD169 at 24, 48, 72, and 96 hpi. Blots were probed for MARCH1, TfR (TB40/E only), IE1, IE2, pp28, and the loading control p115. (F) qPCR analysis of MARCH1 transcripts isolated from fibroblasts infected with wild-type TB40/E (WT) or a UL111A-STOP virus at 96 hpi. Results reported as the number of transcripts as normalized to GAPDH. (G) qPCR analysis of cellular IL-10 transcripts isolated from uninfected (UI) or HCMV-infected fibroblasts at 24, 48, 72, 96, and 120 hpi and uninfected (UI) or HCMV-infected (Inf) Kasumi-3 cells. IL-10 transcripts were normalized to GAPDH and reported as a fold change to the uninfected samples. (H) qPCR analysis of MARCH1 transcripts isolated at 96 hpi from HCMV-infected fibroblasts (TB40/E, MOI = 3) treated with DMSO or Acyclovir (Acycl) at 3 hpi. MARCH1 transcripts were normalized to GAPDH and reported as a fold change to the DMSO-treated sample. (I) Western blot analysis for MARCH1, pp28, and the loading control p115 from uninfected fibroblasts or HCMV-infected (WT) fibroblasts treated with DMSO or Acyclovir. For the above panels, * indicates $P < 0.05$, ns = not significant, and data are average of three independent experiments.

many delayed early and late proteins implicated in viral assembly events (pp150, UL71, gB, pp28) were drastically decreased in the absence of MARCH1 (Fig. 3G). This was particularly evident for gB and pp28 and to a lesser extent for pp150 and UL71. The decrease in protein correlated with a decrease in transcripts, as pp28, but not IE transcripts, were reduced in the infection of the knockdown cells (Fig. 3H). Thus, the absence of MARCH1 results in a general block in the late stages of HCMV infection.

We next performed immunofluorescence (IF) and electron microscopy analyses. By immunofluorescence analysis we observed reduced staining of pp28, consistent with the western analysis, and found that the reduced pp28 that was produced was not

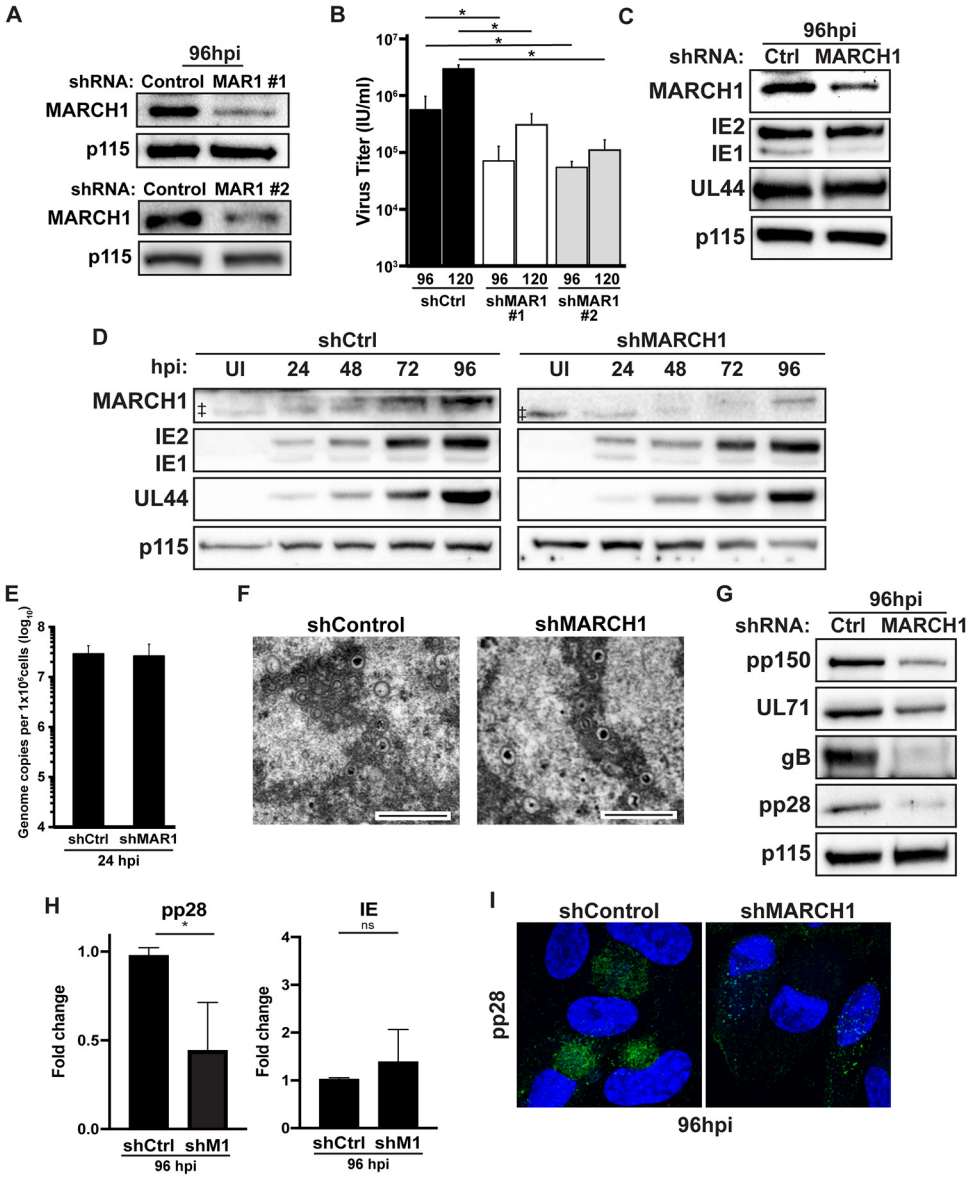

FIG 3 MARCH1 knockdown reduces HCMV titers. (A) Western blot analysis for MARCH1 and p115 loading control at 96 hpi in fibroblasts infected with HCMV (TB40/E strain, MOI = 3) and expressing a scrambled shRNA or shRNA against MARCH1. (B) Infectious titers at 96 and 120 hpi from HCMV-infected fibroblasts expressing a scrambled shRNA or shRNA against MARCH1. (C) Western blot analysis from HCMV-infected (96 hpi) fibroblasts expressing a scrambled shRNA or an shRNA against MARCH1. Blots were probed for MARCH1, IE1, IE2, UL44, and the loading control p115. (D) Western blot analysis of lysates from uninfected or infected cells as described in (C) harvested at 24, 48, 72, and 96 hpi. ‡ indicates nonspecific band (E) HCMV genome copies at 24 hpi in control or MARCH1 knockdown fibroblasts. (F) EM images from nuclei of infected control or MARCH1 knockdown fibroblasts at 96 hpi. Scale bar: 500 nm. (G) Western blot analysis of lysates as described in (C). Blots were probed for pp150, UL71, gB, pp28, and the loading control p115. (H) qPCR analysis of IE1 and pp28 transcripts isolated from control or MARCH1 knockdown fibroblasts infected with HCMV for 96 h. (I) Immunofluorescent staining for the viral protein pp28 at 96 hpi in control or MARCH1 knockdown fibroblasts infected with HCMV. For the above panels, * indicates $P < 0.05$, ns = not significant, and data are average of three independent experiments.

properly localized to the cVAC (Fig. 3I). This was consistent with EM analysis in which very few virions and dense bodies were present in the cytoplasm of the MARCH1-knockdown cells, although both were prevalent throughout the cytoplasm in the control cells (Fig. 4A and B). One striking observation was that the accumulation of membranes in a juxtanuclear cVAC was apparent in both the control and MARCH1-knockdown infections. We previously reported that the cellular SNARE protein

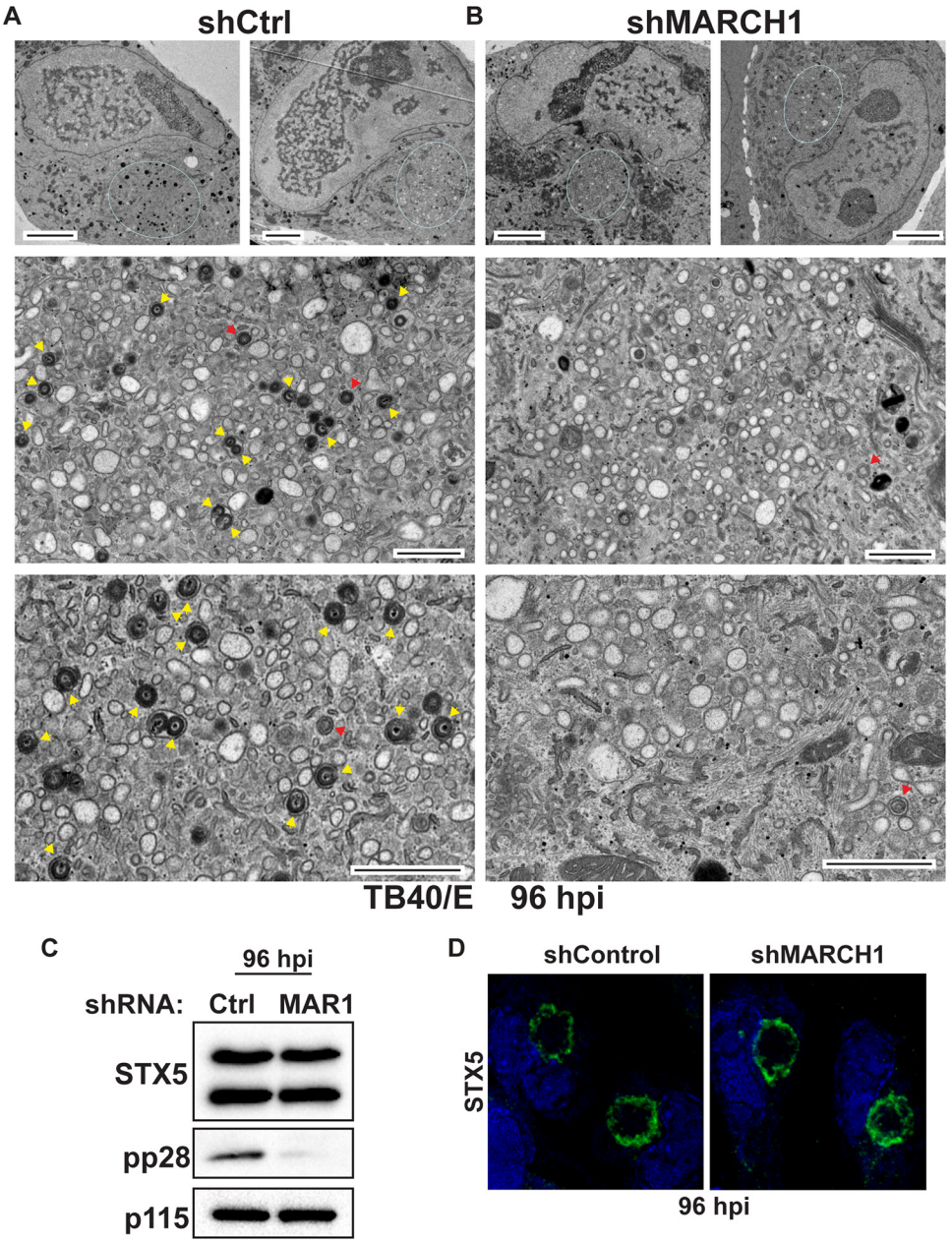

FIG 4 The presence of cytoplasmic virions is reduced in the absence of MARCH1. Electron micrographs of (A) control and (B) MARCH1 knockdown fibroblasts infected with HCMV (TB40/E strain, MOI = 3) at 96 hpi. The middle and bottom panels are higher magnification images of the cytoplasmic region. Scale bars in upper panels represent 5 μm, and scale bars in middle and lower panels represent 1 μm. Blue circles in upper panels indicate area of membrane accumulation or cVAC. Yellow and red arrows indicate enveloped virions and cytoplasmic A capsids, respectively. (C) Western blot analysis for STX5, pp28, and the loading control p115 from HCMV-infected fibroblasts (TB40/E, MOI = 3) expressing a control shRNA (Ctrl) or shRNA targeting MARCH1 (MAR1). (D) Immunofluorescence images of STX5 (green) at 96 hpi with HCMV TB40/E (MOI = 3) in fibroblasts expressing shRNA control or shRNA targeting MARCH1. Nuclei are stained with DAPI.

Syntaxin 5 (STX5) is induced during infection and is important for the membrane reorganization associated with the cVAC (32). STX5 is induced with similar kinetics as some of the viral proteins whose expression was reduced in the MARCH1-knockdown cells. However, STX5 was still induced and properly localized to the Golgi ring of the cVAC (Fig. 4C & D). Thus, although MARCH1 knockdown has broad effects on the late stages of HCMV infection, not all late events are affected.

MARCH1 knockdown increases iron, lipid peroxidation, and mitochondrial dysfunction. To investigate the hypothesis that MARCH1 downregulates TfR during infection, we checked the levels of TfR during infection of the MARCH1-knockdown fibroblasts. Consistent with the hypothesis, TfR protein was increased in the MARCH1-knockdown cells (Fig. 5A), suggesting that MARCH1 does in fact promote the degradation of TfR during HCMV infection. We found that TfR is internalized late in infection and localizes to a ring around the pp28-containing core of the cVAC. We next wanted to determine if MARCH1 has a similar localization as TfR during the late stages of infection. Lacking a suitable MARCH1 antibody for immunofluorescence, we visualized MARCH1 during infection using a lentivirus expressing EGFP-tagged MARCH1. Previous studies have reported that EGFP tagged to the N-terminus of MARCH1 does not affect the function of the protein (33, 34). At 96 hpi, when the cVAC is fully formed and MARCH1 is highly expressed, EGFP-MARCH1 localized adjacent to the nucleus in a ring-like structure, colocalizing with the Golgi protein STX5 (Fig. 5B). While coexpression of the EGFP-MARCH1 with TfR-mCherry led to a marked reduction in the TfR signal, likely due to March1-induced degradation, colocalization of TfR and MARCH1 was apparent (Fig. 5C).

If the role of MARCH1 during HCMV infection is to degrade TfR, we hypothesize that iron levels will be elevated during infection of the MARCH1-knockdown cells. Accordingly, we found an increase in the LIP in MARCH1-knockdown fibroblasts at 96 and 120 hpi (Fig. 5D). The cell has several safeguards to deal with increased cellular iron levels. When these safeguards fail, or are overwhelmed by excess iron, the cell undergoes ferroptosis, an iron-dependent form of cell death distinct from apoptosis and necroptosis (35). One safeguard against excess iron is the expression of ferritin, which binds to free iron in the cytoplasm and stores it in a nontoxic form. Ferritin consists of 24 subunits of two species, heavy (FTH) (21 kDa) and light (19 kDa), that are highly homologous (36). We found that FTH was drastically reduced during infection and did not increase upon knockdown of MARCH1 (Fig. 5E). Thus, ferritin was not present to safeguard against the increase in iron observed upon MARCH1 knockdown.

The presence of excess iron in the cell leads to lipid peroxidation and ferroptosis. The cell protects against lipid peroxidation via glutathione-dependent antioxidant defenses. For example, the cellular protein GPX4 can counter lipid peroxidation by utilizing glutathione or other thiols to reduce key intermediates in the lipid peroxidase chain reaction (37). However, we found that similar to ferritin, levels of GPX4 are reduced during infection and do not recover when MARCH1 is knocked down (Fig. 5E). Malondialdehyde (MDA) is one of the most commonly used biomarkers for lipid peroxidation, and we found levels of MDA to be significantly increased following infection (Fig. 5F). This may be a result of the observed downregulation of GPX4 during infection. We found an additional increase in MDA levels when MARCH1 is knocked down (Fig. 5F), which is consistent with the increase in cytoplasmic iron combined with the absence of the ferritin and GPX4 safeguards that are downregulated during infection. Thus, taken in sum, while the cell has several safeguards to deal with elevated iron levels, many of the important proteins involved in these checks are downregulated during infection, thus rendering the cell more susceptible to conditions that increase cellular iron.

One hallmark of the induction of ferroptosis is the depolarization of mitochondrial membranes. Infection results in a slight, but significant, increase in mitochondrial depolarization. In the absence of MARCH1, there was a three times greater increase in mitochondrial depolarization compared to normal infection (Fig. 5G). Levels of ATP were also significantly reduced during infection of the MARCH1-knockdown fibroblasts (Fig. 5H). The inability to control iron levels during infection adversely affects mitochondrial function and the ability to support a productive infection.

Blocking the early increase in the iron pool reduces infectious HCMV virion production. Our data shows that elevated iron levels late in infection are detrimental to infection. We next wanted to investigate whether the early increase in iron was also required for a productive infection. To assess the role of the early increase in TfR levels,

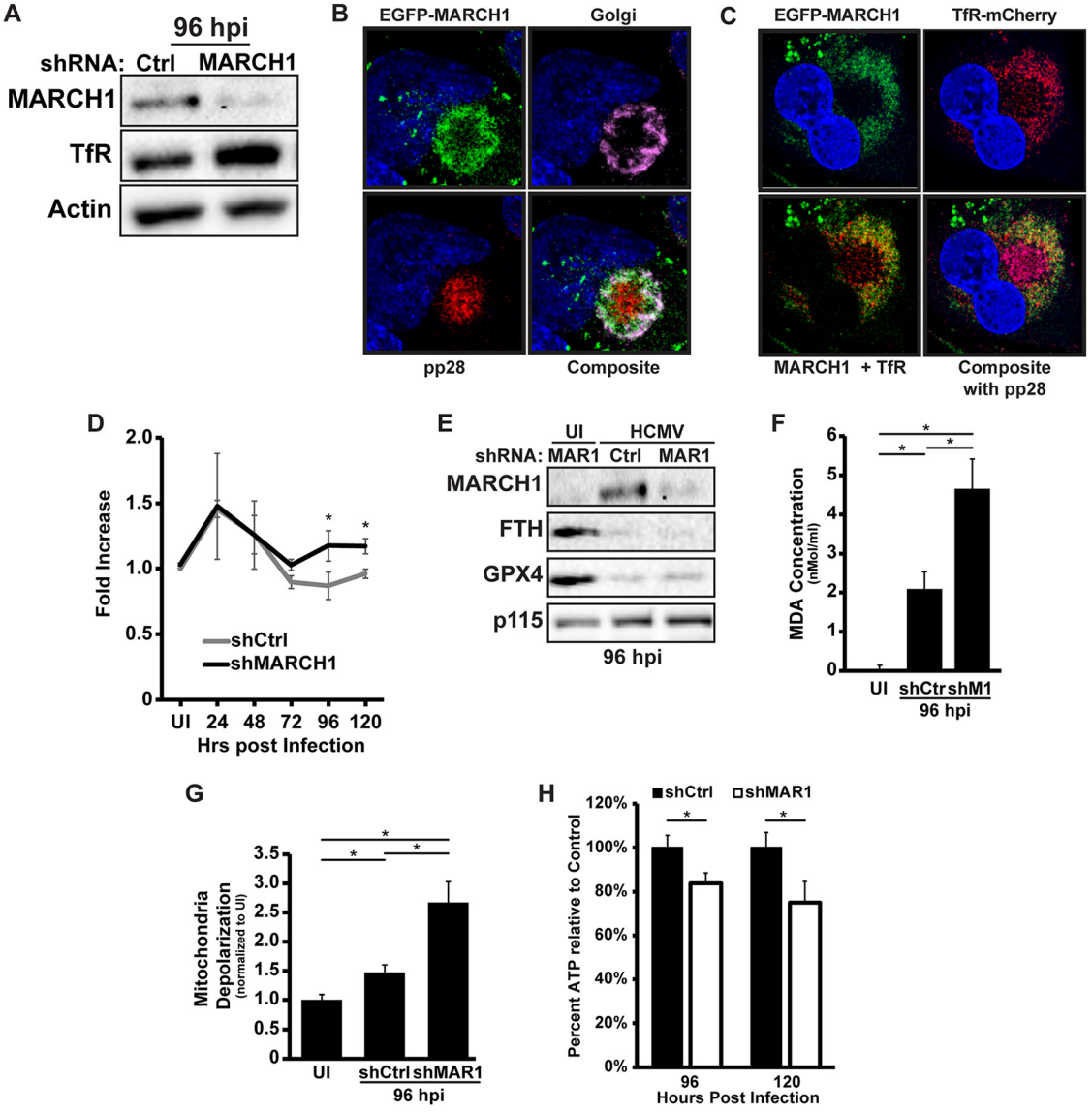

FIG 5 MARCH1 knockdown increases labile iron pool and lipid peroxidation. (A) Western blot analysis at 96 hpi from HCMV-infected (TB40/E, MOI = 3) fibroblasts expressing a scrambled shRNA or an shRNA against MARCH1. Blots were probed for MARCH1, TfR, and the loading control actin. (B) HCMV-infected fibroblasts expressing EGFP-MARCH1 were fixed at 72 hpi and stained for a Golgi marker (pink) and the viral protein pp28 (red). (C) HCMV-infected fibroblasts expressing EGFP-MARCH1 and TfR-mCherry were fixed at 96 hpi and stained for the viral protein pp28 (pink), which is shown only in the composite image. Nuclei in (B) and (C) are stained with DAPI. (D) Labile iron pool measurements taken by measuring calcein fluorescence increase following iron chelation with SIH in uninfected and HCMV-infected (as in (A)) cells expressing a control shRNA (shCtrl) or shRNA against MARCH1 (shMARCH1) at 24, 48, 72, 96, and 120 hpi. Data are presented as fold increase over levels in uninfected shCtrl cells. (E) Western blot analysis from uninfected and HCMV-infected (96 hpi) fibroblasts expressing a control shRNA (Ctrl) or shRNA against MARCH1 (MAR1). Blots were probed for MARCH1, ferritin (FTH), GPX4, and the loading control p115. (F) MDA assay measuring lipid peroxidation in uninfected and HCMV-infected fibroblasts (96 hpi) expressing control shRNA (shCtr) or shRNA against MARCH1 (shM1). (G) Mitochondrial depolarization as measured by JC-10 fluorescence shift in uninfected or HCMV-infected fibroblasts (TB40/E, MOI = 3) expressing control (shCtrl) or MARCH1 shRNA (shMAR1). (H) ATP levels at 96 and 120 hpi in fibroblasts expressing control (shCtrl) or MARCH1 shRNA (shMAR1) infected with HCMV as in (G). For the above panels, * indicates $P < 0.05$ and data are average of three independent experiments.

we infected fibroblasts expressing a control shRNA or shRNA against TfR. We were able to achieve near complete knockdown of TfR using two different clones of shRNA (Fig. 6A). Both clones resulted in greater than a one-log reduction in the production of infectious virions (Fig. 6B). However, we noticed a reduced growth rate and altered morphology in the fibroblasts expressing the TfR shRNA. On occasion, the TfR-knockdown fibroblasts did not survive the selection process, leaving an insufficient number of surviving cells to

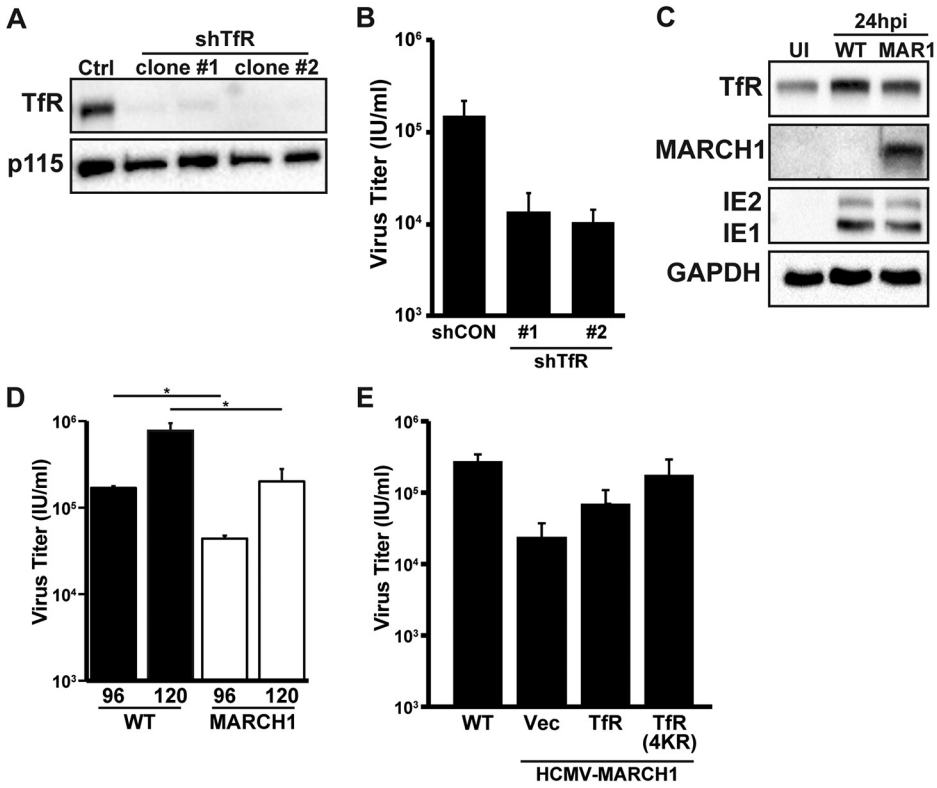

FIG 6 Overexpression of MARCH1 reduces infectious HCMV virion production. (A) Western blot analysis from fibroblasts expressing a scrambled shRNA (Ctrl) or shRNA against TfR. Blots were probed for TfR or p115 loading control. Duplicate samples from two distinct TfR shRNA clones are shown. (B) Infectious titers at 120 hpi from HCMV-infected (TB40/E, MOI = 3) control or TfR knockdown fibroblasts. (C) Western blot analysis for TfR, MARCH1, IE1, IE2, or the loading control GAPDH from fibroblast lysates infected with wild-type HCMV (WT) or HCMV expressing MARCH1 (MAR1) from its genome (MOI = 3, 24 hpi). (D) Infectious titers at 96 hpi and 120 hpi from fibroblasts infected with wild-type HCMV (WT) or HCMV expressing EGFP-MARCH1 from its genome (MOI = 3). (E) Fibroblasts were selected to express a control vector, FKBP-TfR, or FKBP-TfR(4KR) and infected with either wild-type HCMV or HCMV overexpressing MARCH1 (TB40/E, MOI = 3). Infectious titers were assayed at 120 hpi. For the above panels, * indicates $P < 0.05$ and data are average of three independent experiments.

perform infections, and the selection process had to be restarted. Thus, we questioned whether the decreased titers were specifically due to a block in the early rise in TfR during infection and instead wondered if this was a result of an overall decrease in cell fitness and an inability to support a robust infection. An alternative method was therefore required to address whether the early increase in TfR protein was required for infection.

Rather than completely knock down TfR in cells, we sought a method that would allow us to prevent the HCMV-induced transient increased in TfR, while maintaining a protein level close to what is observed in uninfected cells. To do this, we engineered a recombinant HCMV virus with MARCH1 expressed from the US34-TRS1 region within the HCMV genome, a region allowing robust expression of inserted genes (38). Using this virus, we confirmed that MARCH1 was expressed at 24 hpi, resulting in decreased TfR protein levels (Fig. 6C). Thus, any resulting phenotype could be attributed to a block in the TfR increase and not from the adverse cell fitness that occurs when levels of TfR protein are nearly completely abolished. Using this virus, we found a reduction in the production of infectious virions (Fig. 6D). Since the overexpression of MARCH1 may result in the degradation of other MARCH1 targets, therefore either causing or contributing to the observed phenotype, we sought to rescue virus titers by expressing a version of TfR that contains 4 lysine to arginine substitutions (4KR) that prevent its ubiquitination and lysosomal degradation (15). To guard against any adverse effects of prolonged overexpression of TfR, an FKBP death domain was attached at the 5′ end of TfR. This domain results in rapid degradation of the FKBP-TfR protein, which can be stabilized with the addition of

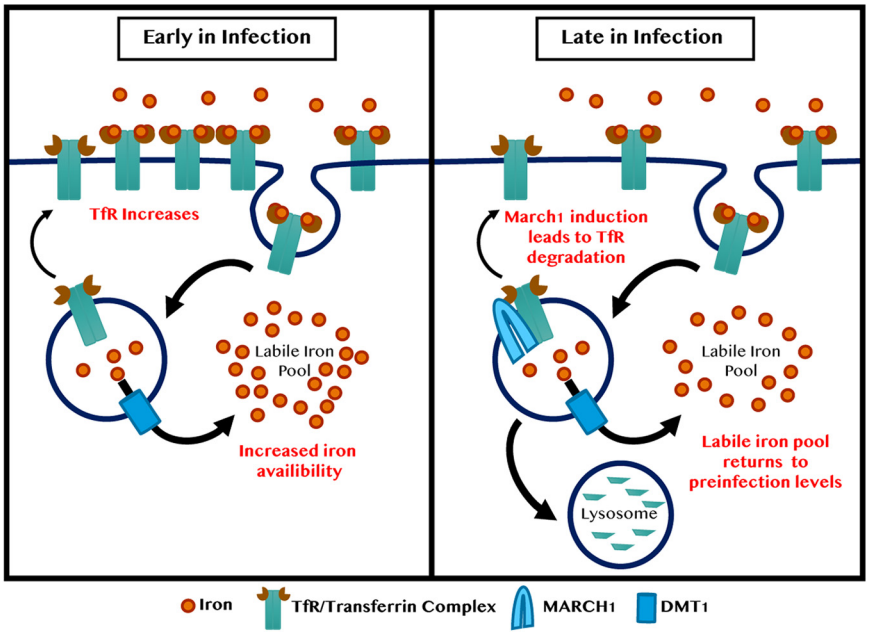

FIG 7 MARCH1 is upregulated to regulate TfR levels and control iron during infection. Model depicting iron levels at early and late times during HCMV infection.

Shield-1. This allowed for a rapid, controlled accumulation of our TfR constructs. While we observed a slight rescue with wild-type TfR, expression of TfR-4KR resulted in titers similar to those observed after infection with wild-type HCMV (Fig. 6E). Therefore, HCMV has changing needs for iron during infection. Dysregulating the iron pools, both early and late in infection, has adverse effects on the ability to produce infectious virions.

DISCUSSION

Under normal conditions, cells tightly regulate the uptake, efflux, and storage of iron. Many proteins are involved in this process, with the Transferrin-TfR complex being a major player in transporting extracellular iron into the cell. HCMV manipulates this process by controlling TfR expression. We found that early in infection TfR expression is increased, leading to increased iron uptake and availability in the cell. There is a transcriptional component to this increase as we observed increased transcripts. From a replication perspective, the virus would benefit from inducing iron uptake during infection as it enhances energy generation and is required for DNA replication (Fig. 7). While iron is beneficial in this way, excess iron can also be damaging, leading to ROS generation and ferroptosis. An alternative explanation to the early increase in iron is that it is a cellular response to infection by increasing toxicity and promoting cell death through ferroptosis. After this initial increase, levels of the LIP are decreased later in infection, which correlates with a decrease in TfR protein. A decrease in the level of TfR transcripts likely contributes to the decline in TfR protein, but it has not yet been determined if this is due to actively repressing transcription or by simply relieving the induction. In addition to modulating transcript levels, we found that a cellular E3 ligase, MARCH1, which targets TfR for lysosomal degradation, is expressed late in infection (Fig. 7). Induction of MARCH1 may occur to counteract the toxic effects of prolonged elevated iron levels, a necessary step to combat toxicity and complete replication, regardless of whether the initial rise in iron was viral-mediated or a host response (Fig. 7).

The discovery that HCMV induces MARCH1 in infected fibroblasts was intriguing since MARCH1 expression is normally restricted to antigen presenting cells. The predominant role of MARCH1 in APCs is to regulate antigen presentation by targeting MHC class II and CD86, essential proteins for T cell activation, for lysosomal degradation (16, 20, 39). MARCH1 therefore modulates the development of immune cells and

regulates immune responses (40–42). Even within these immune cell types, MARCH1 expression is tightly regulated with limited expression under basal conditions (17, 18, 43). The induction of MARCH1 by HCMV is specific to MARCH1, as its homolog MARCH8, while ubiquitously expressed in fibroblasts, is unchanged during infection.

The family of MARCH ubiquitin ligases was originally identified from their homology to the K3 and K5 ligases encoded by another herpesvirus, KSHV (16). Herpes simplex virus-1 and varicella zoster virus both encode RING E3 ubiquitin ligases ICP0 and ORF61, respectively. However, despite a large genome, HCMV does not encode its own E3 ubiquitin ligase, and it is therefore dependent on cellular ligases. We found that MARCH1 plays a proviral role in infection. While MARCH1 is an antiviral factor during HIV-1 infections, a proviral role for its closely related homolog MARCH8 has been described in hepatitis C virus infections (44–46). Even though we focused on the role of MARCH1 in infection, we cannot exclude a contribution from MARCH8, which also targets TfR for degradation. We observed a greater than 90% inhibition of virus production upon knockdown of MARCH1, but it is possible that we would observe a further reduction in infectious titers upon double depletion of MARCH1 and MARCH8.

Several targets of MARCH1 are expressed in fibroblasts, including Fas, CD98, insulin receptor (INSR), stimulator of interferon genes (STING), mitochondrial antiviral signaling protein (MAVS), and TfR (16, 47–49). Proteomics analyses demonstrate that expression of INSR and CD98 remain unchanged during HCMV infection in fibroblasts, suggesting these are not likely targeted by MARCH1 (3). With MARCH1 knockdown, our preliminary analysis did not find an increase in protein levels of Fas, MAVS, or CD98 when compared to the control cells although CD98 did shift in gel mobility. However, further analysis is necessary to determine if MARCH1 regulation of other targets, known or yet to be identified, is important for supporting a productive HCMV infection. We did find that STING expression is also increased in infection when MARCH1 is knocked down. While this presents an interesting implication for MARCH1 regulating the cellular innate immune response, we could not find evidence to support the direct targeting of STING by MARCH1 during HCMV infection. An alternative explanation could be that due to the global block in infection, levels of STING protein were returning to mock levels.

In addition to the changes observed in TfR protein throughout infection, we found that protein levels of the iron storage protein ferritin are downregulated. We also observed a decrease in the levels of the cellular protein GPX4 that prevents the accumulation of lipid peroxides and ferroptosis. The downregulation of these proteins, whether host or viral mediated, alters the ability of the cells to properly deal with variations in levels of iron, as is observed with MARCH1 knockdown. This has therapeutic implications as HCMV-infected cells exhibit a higher susceptibility to iron variation than uninfected cells and infection sensitizes cells to death by ferroptosis in an environment of excess iron. Infection is also adversely affected by depleting iron levels as iron chelators, used for treatment of other conditions, have already been indicated as inhibitors of HCMV infection (11). Our findings highlight the need for iron levels to be tightly regulated to maintain a productive infection, as well as demonstrate that the cell's ability to deal with even the slightest variations in nutrient levels is compromised during infection.

MATERIALS AND METHODS

Cell culture, virus stocks, and infections. Normal human dermal fibroblasts (HDFs) (Cell Applications Inc.), MRC-5 cells (ATCC), and Kasumi-3 cells were cultured as previously described (23). All cytomegalovirus stocks were generated from BACs (50), and recombinants were generated using primers in Table 1. The UL111A-STOP virus is published (23). Recombinant virus sequences were verified by Sanger sequencing (Genewiz). Virus stocks were propagated by electroporating purified BAC DNA into MRC5 cells according to published protocols (51) and titrated by the immunological detection of immediate early proteins as previously described (52, 53).

For HCMV infections, virus was added to HDFs and allowed to incubate for 3 h at 37°C. Cells were washed twice with 1XPBS and replaced with fresh growth medium. Single-step growth curve analysis of all HCMV viruses were performed on HDFs infected at MOI = 3. When applicable, cells were treated with 1 μM aqueous shield-1 (CheminPharma), which stabilizes FKBP(DD)-tagged proteins, at the time of infection. Virus was harvested by scraping cells in the medium, sonicating, vortexing, and centrifuging at 13,000 rpm for 10 min at 4°C. Supernatants were collected, aliquoted, flash frozen in liquid nitrogen, and

TABLE 1 Primers for cloning and qPCR

Name	Sequence
EGFP-MARCH1-galK-For	CCTAGGCTTTTGCAAAAAGCTTGCCACAACCCGGGATCCGCCACCCCTGTTGACAATTAATCATCGGCA
EGFP-MARCH1-galK-Rev	ATGGGTGGCAACTAAAAGGCACAGTCGAGGCTGATCAGCGAGCTCTCAGCACTGTCCTGCTCCTT
EGFP-March1-EGFP-For	CCTAGGCTTTTGCAAAAAGCTTGCCACAACCCGGGATCCGCCACCATGGTGAGCAAGGGCGAGGAGCT GTTCACCGGGGTGGTGCCCATC
EGFP-March1-EGFP-Rev	ATGGGTGGCAACTAAAAGGCACAGTCGAGGCTGATCAGCGAGCTCTCAGACTGATACAACTTCAGGGGG GCCACCCTCTGCAGATGGCAG
GAPDH-For	ACCCACTCCTCCACCTTTGAC
GAPDH-Rev	CTGTTGCTGTAGCCAAATTCGT
MARCH1-For	TCCCAGGAGCCAGTCAAGGTT
MARCH1-Rev	CAAAGCGCAGTGTCCCAGTG
MARCH8-For	ACAGGAAGCCTCCACTTCG
MARCH8-Rev	GACGTGGAATGTCACTGAG
IL-10-For	GGTTGCCAAGCCTTGTCTGA
IL-10-Rev	AGGGAGTTCACATGCGCCT
IE-For	CAAGTCCCGACACGTACC
IE-Rev	TCTGTTTGACGAGTTCTGCCA
pp28-For	GTGTCCCATTCCCGACTCG
pp28-Rev	TTCACAACGTCCACCCACC
TfR-For	CTGCTTTCCCTTTCCTTGCATATT
TfR-Rev	GCTCGTGCCACTTTGTTCAACT
XhoI-March1-For	GCATCTCGAGTAATGACCAGCAGC
BamHI-March1-Rev	GCATGGATCCTCAGACTGATACAACTTC
EcoRI-TfR-For	GCATGAATTCATGATGGATCAAGCTAGATCA
NotI-EGFP-Rev	GCATGCGGCCGCTTACTTGTACAGCTCGTC
BamHI-TfR-Rev	GCATGGATCCTTAAAACTCATTGTCAATGTC
TfR-137-For	GCACAGACTTCACCAGCA
XbaI-FKBP(DD)-For	GCATTCTAGAATGGGAGTGCAGGTGGAA
EcoRI-FKBP(DD)-Rev	GACTGAATTCTTCCGGTTTTAGAAGCTC
β-globin-For	ACGTGGATGAAGTTGGTGGT
β-globin-Rev	GCCCAGTTTCTATTGGTCTCC
4KR Gene block	GCATGAATTCATGATGGATCAAGCTAGATCAGCATTCTCTAACTTGTTTGGTGGAGAACCATTGTCATA TACCCGGTTCAGCCTGGCTCGGCAAGTAGATGGCGATAACAGTCATGTGGAGATGAGGCTTGCTGTA GATGAAGAAGAAAATGCTGACAATAACACAAGGGCCAATGTCACAAGGCCACGGAGGTGTAGTGGA AGTATCTGCTATGGGACTATTGCTGTGATCGTCTTTTTCTTGATTGGATTTATGATTGGCTACTTGGGCT ATTGTAAAGGGGTAGAACCAAAAACTGAGTGTGAGAGACTGGCAGGAACCGAGTCTCCAGTGAGGG AGGAGCCAGGAGAGGACTTCCCTGCAGCACGTCGCTTATATTGGGATGACCTGAAGAGAAAGTTGT CGGAGAAACTGGACAGCACAGACTTCACCAGCACCATCAAGCTGCTGAATG

stored at −80°C until analysis. Samples were titrated by serial dilutions and quantified as described above. Kasumi-3 cells were infected in X-VIVO media as previously described (23).

Lentivirus was generated using the 3rd generation packaging system: pCMV-VSV-G (gift from Bob Weinberg, Addgene #8454), pMDLg-RRE (gift from Didier Trono, Addgene #12251), and pRSV-Rev (gift from Didier Trono, Addgene #12253) as described previously (54). The MARCH1 (TRCN0000037019 (clone #1), TRCN0000037021 (clone #2)) and TfR (TRCN0000057658 (clone #1), TRCN0000057659 (clone #2)) shRNA plasmids were from the TRC1.0 shRNA library. Scrambled control was a gift from David Sabatini (Addgene #1864). The puro sequence was replaced with a puro-2A-EGFP sequence by generating the T2A-EGFP insert by PCR and fusing it to the end of the puromycin without a stop codon using gene sewing technique. Restriction sequences for BamHI and KpnI were introduced and used for cloning into the corresponding sites on the designated pLKO.1 plasmids. Primers used for all cloning are listed in Table 1. The MARCH1 sequence was amplified from pCDNA3.1-MARCH1-EYFP (gift from Dr. Jacques Thibodeau) and inserted into the XhoI/BamHI sites on pEGFPC1. EGFP-MARCH1 was transferred to pCDH-CMV-MCS-EF1-Puro (System Biosciences) using NheI/BamHI sites to generate pCDH-EGFP-MARCH1. The TfR-EGFP sequence was amplified from pBA-TfR-EGFP (gift from Gary Banker and Marvin Bentley (55), Addgene #45060) and ligated into pCDH-CMV-MCS-EF1-Puro using EcoRI/NotI sites. The EGFP was replaced with mCherry using BamHI/NotI sites to generate pCDH-TfR-mCherry. The death domain sequence from FKBP was amplified from pBMN-FKBP(DD)-YFP (gift from Thomas Wandless (56), Addgene #31763) with primers containing XbI and EcoRI and inserted into pCDH using the corresponding sites to generate pCDH-FKBP(DD). The TfR-sequence was subsequently amplified using primers that added EcoRI and BamHI sites to the 5′ and 3′ ends, respectively, and inserted at the 3′ of FKBP(DD) using the aforementioned sites to generate pCDH-FKBP(DD)-TfR. The first 445 nucleotides of TfR were synthesized (Integrated DNA Technologies) with mutations to encode arginine at positions K39, K53,

TABLE 2 Primary antibodies

Target	Source	Assay[a]	Target	Source	Assay[a]
IE1/2	(53)	W	MARCH1	MilliporeSigma	W
IE1/2 (ex2/3)	Jim Alwine (60)	W, IF	STX5	Santa Cruz	W
UL71	(23)	W	STX5	Synaptic Systems	IF
pp150	Bill Britt	W	FTH	CellSignaling	W
pp28	Virusys	W, IF	GPX4	CellSignaling	W
gB	Virusys	W	p115	Proteintech	W
UL44	Santa Cruz	W	Actin	MilliporeSigma	W
TfR	CellSignaling	W	GAPDH	Santa Cruz	W

[a]IF, immunofluorescence; W, Western blot.

K58, and K60. The remaining TfR sequence was amplified using a primer that generated a 5′ 36 bp overlap with the 3′ end of the synthesized 4KR construct. This PCR product and the 4KR fragment were stitched together using PCR primers containing EcoRI and BamHI. The resulting TfR(4KR) sequence was inserted into the pCDH-FKBP(DD) using the respective EcoRI and BamHI sites to generate pCDH-FKBP (DD)-TfR(4KR).

For lentivirus transduction, subconfluent fibroblasts were seeded overnight and transduced with lentivirus and 8 μg/mL Polybrene (Sigma-Aldrich). Transduced cells were selected using 2 μg/mL puromycin (Thermo Fisher) and before seeding for HCMV infection as described above.

Western blotting. Western blots and cell lysate harvests were performed as previously described (54). Where applicable, 50 μM chloroquine (MilliporeSigma) or 0.5 μM concanamycin A (Santa Cruz) was added 24 h before harvest or 100 μg/mL acyclovir (EMD Millipore) was added at the time of infection. The primary antibodies are listed in Table 2. The horseradish peroxidase-conjugated secondary antibodies were from GE Healthcare. Blots were developed with SuperSignal West Pico PLUS Chemiluminescent Substrate (Thermo Fisher Scientific). Bands from three independent samples were quantified using ImageLab densitometry.

Immunofluorescence microscopy and imaging. Fibroblasts were grown on coverslips and infected with HCMV as described above. Cells were fixed with 4% paraformaldehyde for 15 min at room temperature and blocked in PBS containing 10% human serum, 0.5% Tween 20, and 5% glycine. Triton X-100 (0.1%) was added for permeabilization. Primary antibodies are listed in Table 2. Mouse or rabbit secondary antibodies were Alexa Fluor 488, 568, and 647 (Thermo Fisher Scientific). Coverslips were mounted with ProLong Diamond Antifade Mountant with DAPI (ThermoFisher). Images were taken on a C2+ Confocal Microscope System (Nikon). Images were processed using NIS elements software and are either a single slice of a Z-stack or a volume rendering of the Z-stacks.

Reverse transcriptase and quantitative PCR. At indicated time points, RNA was isolated from cells using RNeasy minikit (Qiagen) following manufacturer's protocol. RNA concentration was quantified using NanoDrop 2000 (ThermoFisher), and cDNA was synthesized using SuperScript first-strand synthesis system for RT-PCR (ThermoFisher) following manufacturer's protocol. Samples were cycled on a StepOnePlus real-time PCR system (ThermoFisher): 50°C 2 min, 95°C 10 min, (95°C 15 sec, 60°C 60 sec, 55°C 30 sec, 40 cycles). Primers are listed in Table 1. Data were analyzed using delta-Ct method with GAPDH as normalization control. To calculate absolute transcript numbers, standard curves for each primer set were generated by dilution series (1 ng to 1fg). Samples from RT-PCR were run on 4% agarose gel for visualization.

Electron microscopy. Fibroblasts expressing MARCH1- and scrambled-shRNA were seeded in 60 mm Permanox tissue culture dishes (Nalge Nunc International) and were infected as described above. Cells were washed two times with 1XPBS and fixed in fixation buffer (0.5% vol/vol glutaraldehyde, 0.04% vol/vol paraformaldehyde, 0.1M sodium cacodylate) for 1 h at 4°C at 96 hpi. Cells were processed by the Microscopy Imaging Facility at Penn State College of Medicine. Briefly, the fixed samples were washed three times with 0.1M sodium cacodylate, followed by postfixation in 1% osmium–1.5% potassium ferrocyanide overnight at 4°C. Samples were washed 3 times in 0.1M sodium cacodylate, dehydrated with ethanol, and embedded in Epon 812 for staining and sectioning. Images were acquired using a JEOL JEM-1400 Digital Capture transmission electron microscope.

Viral DNA replication. Fibroblasts were infected as described above and harvested at 24 hpi. DNA was isolated using a DNeasy blood and tissue kit (Qiagen). Quantitative PCR (qPCR) was performed on the extracted DNA using the primers in Table 1. To generate a standard curve for UL99 and β-globin,10-fold dilutions of respective sequences were subjected to qPCR analysis. UL99 genomic equivalents were normalized to the β-globin.

Calcein labile iron pool assay. The intracellular LIP was determined as previously described (57–59). HDFs were washed with PBS, then incubated with calcein-AM (25 μM) (Cayman) in 1XPBS with 1 mg/mL BSA and 20 mM HEPES at 37°C for 15 min. After loading, cells were washed with PBS and incubated in 1XPBS with 1 mg/mL BSA and 20 mM HEPES for 30 min at 37°C to allow calcein fluorescence to stabilize. Fluorescence was measured with a Synergy H1 hybrid reader at 37°C (488/517). Iron-bound calcein was determined by adding the cell-permeant iron chelator, isonicotinoyl salicylaldehyde hydrazone (SIH) (Cayman) at 100 μM and measuring fluorescence after 2-min incubation. The fluorescence difference after the addition of SIH was normalized to uninfected cells at each time point.

CellTiter-Glo, lipid peroxidation, mitochondrial membrane potential (MMP) assays. ATP levels were evaluated with the CellTiter-Glo cell viability assay (Promega) following the manufacturer's instructions. Lipid peroxidation was evaluated by measuring malondialdehyde (MDA) using a Lipid Peroxidation (MDA) assay kit (MilliporeSigma) following the manufacturer's protocol. MMP was measured using the fluorophore JC-10 (AdipoGen). HDFs cultured in black 96-well plates were washed with 1XPBS, then incubated with 1 μM JC-10 for 30 min at 37°C, followed by another wash with 1XPBS. Fluorescence intensity was measured at both 480/525 and 540/590 with the Synergy H1 hybrid reader, and the ratio of green to red fluorescence was calculated.

ACKNOWLEDGMENTS

We thank Natalie Buchkovich and Alexandria Ostman for technical assistance. We thank Han Chen of the Penn State College of Medicine TEM core for assistance with processing samples for electron microscopy.

REFERENCES

1. Griffiths PD. 2012. Burden of disease associated with human cytomegalovirus and prospects for elimination by universal immunisation. Lancet Infect Dis 12:790–798. https://doi.org/10.1016/S1473-3099(12)70197–4.
2. Griffiths P, Baraniak I, Reeves M. 2015. The pathogenesis of human cytomegalovirus. J Pathol 235:288–297. https://doi.org/10.1002/path.4437.
3. Weekes MP, Tomasec P, Huttlin EL, Fielding CA, Nusinow D, Stanton RJ, Wang ECY, Aicheler R, Murrell I, Wilkinson GWG, Lehner PJ, Gygi SP. 2014. Quantitative temporal viromics: an approach to investigate host-pathogen interaction. Cell 157:1460–1472. https://doi.org/10.1016/j.cell.2014.04.028.
4. Munger J, Bajad SU, Coller HA, Shenk T, Rabinowitz JD. 2006. Dynamics of the cellular metabolome during human cytomegalovirus infection. PLoS Pathog 2:e132. https://doi.org/10.1371/journal.ppat.0020132.
5. Drakesmith H, Prentice A. 2008. Viral infection and iron metabolism. Nat Rev Microbiol 6:541–552. https://doi.org/10.1038/nrmicro1930.
6. Wang J, Pantopoulos K. 2011. Regulation of cellular iron metabolism. Biochem J 434:365–381. https://doi.org/10.1042/BJ20101825.
7. Kruszewski M. 2003. Labile iron pool: the main determinant of cellular response to oxidative stress. Mutat Res 531:81–92. https://doi.org/10.1016/j.mrfmmm.2003.08.004.
8. Jiang X, Stockwell BR, Conrad M. 2021. Ferroptosis: mechanisms, biology and role in disease. Nat Rev Mol Cell Biol 22:266–282. https://doi.org/10.1038/s41580-020–00324-8.
9. Vogel J-U, Schmidt S, Schmidt D, Rothweiler F, Koch B, Baer P, Rabenau H, Michel D, Stamminger T, Michaelis M, Cinatl J. 2019. The thrombopoietin receptor agonist eltrombopag inhibits human cytomegalovirus replication via iron chelation. Cells 9:31. https://doi.org/10.3390/cells9010031.
10. Crowe WE, Maglova LM, Ponka P, Russell JM. 2004. Human cytomegalovirus-induced host cell enlargement is iron dependent. Am J Physiol Cell Physiol 287:C1023–C1030. https://doi.org/10.1152/ajpcell.00511.2003.
11. Cinatl J, Cinatl J, Rabenau H, Gümbel HO, Kornhuber B, Doerr HW, Jr. 1994. In vitro inhibition of human cytomegalovirus replication by desferrioxamine. Antiviral Res 25:73–77. https://doi.org/10.1016/0166–3542(94)90095–7.
12. Cinatl J, Hoffmann F, Cinatl J, Weber B, Scholz M, Rabenau H, Stieneker F, Kabickova H, Blasko M, Doerr HW. 1996. In vitro inhibition of human cytomegalovirus replication by calcium trinatrium diethylenetriaminepentaacetic acid. Antiviral Res 31:23–34. https://doi.org/10.1016/0166–3542(95)00833–0.
13. Ben-Arieh SV, Zimerman B, Smorodinsky NI, Yaacubovicz M, Schechter C, Bacik I, Gibbs J, Bennink JR, Yewdell JW, Coligan JE, Firat H, Lemonnier F, Ehrlich R. 2001. Human cytomegalovirus protein US2 interferes with the expression of human HFE, a nonclassical class I major histocompatibility complex molecule that regulates iron homeostasis. J Virol 75:10557–10562. https://doi.org/10.1128/JVI.75.21.10557–10562.2001.
14. Tachiyama R, Ishikawa D, Matsumoto M, Nakayama KI, Yoshimori T, Yokota S, Himeno M, Tanaka Y, Fujita H. 2011. Proteome of ubiquitin/MVB pathway: possible involvement of iron-induced ubiquitylation of transferrin receptor in lysosomal degradation. Genes Cells 16:448–466. https://doi.org/10.1111/j.1365–2443.2011.01499.x.
15. Fujita H, Iwabu Y, Tokunaga K, Tanaka Y. 2013. Membrane-associated RING-CH (MARCH) 8 mediates the ubiquitination and lysosomal degradation of the transferrin receptor. J Cell Sci 126(Pt 13):2798–2809.
16. Bartee E, Mansouri M, Hovey Nerenberg BT, Gouveia K, Früh K. 2004. Downregulation of major histocompatibility complex class I by human ubiquitin ligases related to viral immune evasion proteins. J Virol 78:1109–1120. https://doi.org/10.1128/jvi.78.3.1109–1120.2004.
17. Matsuki Y, Ohmura-Hoshino M, Goto E, Aoki M, Mito-Yoshida M, Uematsu M, Hasegawa T, Koseki H, Ohara O, Nakayama M, Toyooka K, Matsuoka K, Hotta H, Yamamoto A, Ishido S. 2007. Novel regulation of MHC class II function in B cells. EMBO J 26:846–854. https://doi.org/10.1038/sj.emboj.7601556.
18. De Gassart A, Camosseto V, Thibodeau J, Ceppi M, Catalan N, Pierre P, Gatti E. 2008. MHC class II stabilization at the surface of human dendritic cells is the result of maturation-dependent MARCH I down-regulation. Proc Natl Acad Sci U S A 105:3491–3496. https://doi.org/10.1073/pnas.0708874105.
19. Thibodeau J, Bourgeois-Daigneault M-C, Huppé G, Tremblay J, Aumont A, Houde M, Bartee E, Brunet A, Gauvreau M-E, de Gassart A, Gatti E, Baril M, Cloutier M, Bontron S, Früh K, Lamarre D, Steimle V. 2008. Interleukin-10-induced MARCH1 mediates intracellular sequestration of MHC class II in monocytes. Eur J Immunol 38:1225–1230. https://doi.org/10.1002/eji.200737902.
20. Ohmura-Hoshino M, Matsuki Y, Aoki M, Goto E, Mito M, Uematsu M, Kakiuchi T, Hotta H, Ishido S. 2006. Inhibition of MHC class II expression and immune responses by c-MIR. J Immunol 177:341–354. https://doi.org/10.4049/jimmunol.177.1.341.
21. Goto E, Ishido S, Sato Y, Ohgimoto S, Ohgimoto K, Nagano-Fujii M, Hotta H. 2003. c-MIR, a human E3 ubiquitin ligase, is a functional homolog of herpesvirus proteins MIR1 and MIR2 and has similar activity. J Biol Chem 278:14657–14668. https://doi.org/10.1074/jbc.M211285200.
22. Galbas T, Steimle V, Lapointe R, Ishido S, Thibodeau J. 2012. MARCH1 down-regulation in IL-10-activated B cells increases MHC class II expression. Cytokine 59:27–30. https://doi.org/10.1016/j.cyto.2012.03.015.
23. Sandhu P, and, Buchkovich NJ. 2020. HCMV decreases MHC class II by regulating CIITA transcript levels in a myeloid cell line. J Virol 94:e01901-19. https://doi.org/10.1128/JVI.01901-19.
24. Das S, Vasanji A, Pellett PE. 2007. Three-dimensional structure of the human cytomegalovirus cytoplasmic virion assembly complex includes a reoriented secretory apparatus. J Virol 81:11861–11869. https://doi.org/10.1128/JVI.01077–07.
25. Das S, Pellett PE. 2011. Spatial relationships between markers for secretory and endosomal machinery in human cytomegalovirus-infected cells versus those in uninfected cells. J Virol 85:5864–5879. https://doi.org/10.1128/JVI.00155–11.
26. Sanchez V, Greis KD, Sztul E, Britt WJ. 2000. Accumulation of virion tegument and envelope proteins in a stable cytoplasmic compartment during human cytomegalovirus replication: characterization of a potential site of virus assembly. J Virol 74:975–986. https://doi.org/10.1128/jvi.74.2.975–986.2000.
27. Dautry-Varsat A, Ciechanover A, Lodish HF. 1983. pH and the recycling of transferrin during receptor-mediated endocytosis. Proc Natl Acad Sci U S A 80:2258–2262. https://doi.org/10.1073/pnas.80.8.2258.
28. Omary MB, Trowbridge IS. 1981. Biosynthesis of the human transferrin receptor in cultured cells. J Biol Chem 256:12888–12892. https://doi.org/10.1016/S0021-9258(18)42979–1.
29. Enns CA, Mulkins MA, Sussman H, Root B. 1988. Modulation of the transferrin receptor during DMSO-induced differentiation in HL-60 cells. Exp Cell Res 174:89–97. https://doi.org/10.1016/0014–4827(88)90144–9.

30. Rutledge EA, Mikoryak CA, Draper RK. 1991. Turnover of the transferrin receptor is not influenced by removing most of the extracellular domain. J Biol Chem 266:21125–21130. https://doi.org/10.1016/S0021-9258(18)54829–8.
31. Poole E, Lau JCH, Sinclair J. 2015. Latent infection of myeloid progenitors by human cytomegalovirus protects cells from FAS-mediated apoptosis through the cellular IL-10/PEA-15 pathway. J Gen Virol 96:2355–2359. https://doi.org/10.1099/vir.0.000180.
32. Cruz L, Streck NT, Ferguson K, Desai T, Desai DH, Amin SG, Buchkovich NJ. 2017. Potent inhibition of human cytomegalovirus by modulation of cellular SNARE syntaxin 5. J Virol 91: e01637-16. https://doi.org/10.1128/JVI.01637–16.
33. Bourgeois-Daigneault MC, Thibodeau J. 2012. Autoregulation of MARCH1 expression by dimerization and autoubiquitination. J Immunol 188: 4959–4970. https://doi.org/10.4049/jimmunol.1102708.
34. Bourgeois-Daigneault MC, Thibodeau J. 2013. Identification of a novel motif that affects the conformation and activity of the MARCH1 E3 ubiquitin ligase. J Cell Sci 126(4):989–998.
35. Dixon SJ, Lemberg KM, Lamprecht MR, Skouta R, Zaitsev EM, Gleason CE, Patel DN, Bauer AJ, Cantley AM, Yang WS, Morrison B, Stockwell BR. 2012. Ferroptosis: an iron-dependent form of nonapoptotic cell death. Cell 149: 1060–1072. https://doi.org/10.1016/j.cell.2012.03.042.
36. Arosio P, Adelman TG, and, Drysdale JW. 1978. On ferritin heterogeneity: further evidence for heteropolymers. J Biol Chem 253:4451–4458. https://doi.org/10.1016/S0021-9258(17)34741–5.
37. Yang WS, SriRamaratnam R, Welsch ME, Shimada K, Skouta R, Viswanathan VS, Cheah JH, Clemons PA, Shamji AF, Clish CB, Brown LM, Girotti AW, Cornish VW, Schreiber SL, Stockwell BR. 2014. Regulation of ferroptotic cancer cell death by GPX4. Cell 156:317–331. https://doi.org/10.1016/j.cell.2013.12.010.
38. O'Connor CM, Shenk T. 2011. Human cytomegalovirus pUS27 G protein-coupled receptor homologue is required for efficient spread by the extracellular route but not for direct cell-to-cell spread. J Virol 85: 3700–3707. https://doi.org/10.1128/JVI.02442–10.
39. Ohmura-Hoshino M, Matsuki Y, Mito-Yoshida M, Goto E, Aoki-Kawasumi M, Nakayama M, Ohara O, Ishido S. 2009. Cutting edge: requirement of MARCH-I-mediated MHC II ubiquitination for the maintenance of conventional dendritic cells. J Immunol 183:6893–6897. https://doi.org/10.4049/jimmunol.0902178.
40. Oh J, Wu N, Baravalle G, Cohn B, Ma J, Lo B, Mellman I, Ishido S, Anderson M, Shin J-S. 2013. MARCH1-mediated MHCII ubiquitination promotes dendritic cell selection of natural regulatory T cells. J Exp Med 210: 1069–1077. https://doi.org/10.1084/jem.20122695.
41. Kishta OA, Sabourin A, Simon L, McGovern T, Raymond M, Galbas T, Majdoubi A, Ishido S, Martin J, Thibodeau J. 2018. March1 E3 ubiquitin ligase modulates features of allergic asthma in an ovalbumin-induced mouse model of lung inflammation. J Immunol Res 2018:3823910. https://doi.org/10.1155/2018/3823910.
42. Galbas T, Raymond M, Sabourin A, Bourgeois-Daigneault M-C, Guimont-Desrochers F, Yun TJ, Cailhier J-F, Ishido S, Lesage S, Cheong C, Thibodeau J. 2017. MARCH1 E3 ubiquitin ligase dampens the innate inflammatory response by modulating monocyte functions in mice. J Immunol 198:852–861. https://doi.org/10.4049/jimmunol.1601168.
43. Jabbour M, Campbell EM, Fares H, Lybarger L. 2009. Discrete domains of MARCH1 mediate its localization, functional interactions, and posttranscriptional control of expression. J Immunol 183:6500–6512. https://doi.org/10.4049/jimmunol.0901521.
44. Tada T, Zhang Y, Koyama T, Tobiume M, Tsunetsugu-Yokota Y, Yamaoka S, Fujita H, Tokunaga K. 2015. MARCH8 inhibits HIV-1 infection by reducing virion incorporation of envelope glycoproteins. Nat Med 21:1502–1507. https://doi.org/10.1038/nm.3956.
45. Zhang Y, Tada T, Ozono S, Yao W, Tanaka M, Yamaoka S, Kishigami S, Fujita H, Tokunaga K. 2019. Membrane-associated RING-CH (MARCH) 1 and 2 are MARCH family members that inhibit HIV-1 infection. J Biol Chem 294:3397–3405. https://doi.org/10.1074/jbc.AC118.005907.
46. Kumar S, Barouch-Bentov R, Xiao F, Schor S, Pu S, Biquand E, Lu A, Lindenbach BD, Jacob Y, Demeret C, Einav S. 2019. MARCH8 ubiquitinates the Hepatitis C virus nonstructural 2 protein and mediates viral envelopment. Cell Rep 26:1800–1814.e5. https://doi.org/10.1016/j.celrep.2019.01.075.
47. Wu J, Xia L, Yao X, Yu X, Tumas KC, Sun W, Cheng Y, He X, Peng YC, Singh BK, Zhang C, Qi CF, Bolland S, Best SM, Gowda C, Huang R, Myers TG, Long CA, Wang RF, Su XZ. 2020. The E3 ubiquitin ligase MARCH1 regulates antimalaria immunity through interferon signaling and T cell activation. Proc Natl Acad Sci U S A 117:16567–16578. https://doi.org/10.1073/pnas.2004332117.
48. Eyster CA, Cole NB, Petersen S, Viswanathan K, Früh K, Donaldson JG. 2011. MARCH ubiquitin ligases alter the itinerary of clathrin-independent cargo from recycling to degradation. Mol Biol Cell 22:3218–3230. https://doi.org/10.1091/mbc.E10-11–0874.
49. Nagarajan A, Petersen MC, Nasiri AR, Butrico G, Fung A, Ruan H-B, Kursawe R, Caprio S, Thibodeau J, Bourgeois-Daigneault M-C, Sun L, Gao G, Bhanot S, Jurczak MJ, Green MR, Shulman GI, Wajapeyee N. 2016. MARCH1 regulates insulin sensitivity by controlling cell surface insulin receptor levels. Nat Commun 7:12639. https://doi.org/10.1038/ncomms12639.
50. Warming S, Costantino N, Court DL, Jenkins NA, Copeland NG. 2005. Simple and highly efficient BAC recombineering using galK selection. Nucleic Acids Res 33:e36. https://doi.org/10.1093/nar/gni035.
51. Spector DJ, and, Yetming K. 2010. UL84-independent replication of human cytomegalovirus strain TB40/E. Virology 407:171–177. https://doi.org/10.1016/j.virol.2010.08.029.
52. Britt WJ. 2010. Human cytomegalovirus: propagation, quantification, and storage. Curr Protoc Microbiol Chapter 14:Unit 14E.3. https://doi.org/10.1002/9780471729259.mc14e03s18.
53. Desai D, Lauver M, Ostman A, Cruz L, Ferguson K, Jin G, Roper B, Brosius D, Lukacher A, Amin S, Buchkovich N. 2019. Inhibition of diverse opportunistic viruses by structurally optimized retrograde trafficking inhibitors. Bioorg Med Chem 27:1795–1803. https://doi.org/10.1016/j.bmc.2019.03.026.
54. Streck NT, Carmichael J, Buchkovich NJ. 2018. Nonenvelopment role for the ESCRT-III complex during human cytomegalovirus infection. J Virol 92:e02096-17. https://doi.org/10.1128/JVI.02096–17.
55. Burack MA, Silverman MA, Banker G. 2000. The role of selective transport in neuronal protein sorting. Neuron 26:465–472. https://doi.org/10.1016/S0896-6273(00)81178–2.
56. Banaszynski LA, Chen L-C, Maynard-Smith LA, Ooi AGL, Wandless TJ. 2006. A rapid, reversible, and tunable method to regulate protein function in living cells using synthetic small molecules. Cell 126:995–1004. https://doi.org/10.1016/j.cell.2006.07.025.
57. Ternes N, Scheiber-Mojdehkar B, Landgraf G, Goldenberg H, Sturm B. 2007. Iron availability and complex stability of iron hydroxyethyl starch and iron dextran a comparative in vitro study with liver cells and macrophages. Nephrol Dial Transplant 22:2824–2830. https://doi.org/10.1093/ndt/gfm315.
58. Sturm B, Goldenberg H, Scheiber-Mojdehkar B. 2003. Transient increase of the labile iron pool in HepG2 cells by intravenous iron preparations. Eur J Biochem 270:3731–3738. https://doi.org/10.1046/j.1432–1033.2003.03759.x.
59. Tenopoulou M, Kurz T, Doulias P-T, Galaris D, Brunk UT. 2007. Does the calcein-AM method assay the total cellular "labile iron pool" or only a fraction of it? Biochem J 403:261–266. https://doi.org/10.1042/BJ20061840.
60. Harel NY, Alwine JC. 1998. Phosphorylation of the human cytomegalovirus 86-kilodalton immediate-early protein IE2. J Virol 72:5481–5492. https://doi.org/10.1128/JVI.72.7.5481–5492.1998.